Electronic Supplementary Information

High performance self-charging supercapacitor using porous PVDF-ionic liquid electrolyte sandwiched between two-dimensional graphene electrodes

Surjit Sahoo[a, #], Karthikeyan Krishnamoorthy[a, #], Parthiban Pazhamalai[a], Vimal Kumar Mariappan[a], Sindhuja Manoharan[a], and Sang-Jae Kim[a, b*]

[a]Nanomaterials & System Lab, Department of Mechatronics Engineering, Jeju National University, Jeju 63243, South Korea.

[b]Department of Advanced Convergence Science and Technology, Jeju National University, Jeju 63243, South Korea.

[#]These authors contributed equally.

*Corresponding author. Email: kimsangj@jejunu.ac.kr

1. Experimental section

1.1 Materials

Graphite powder and polyvinylidene fluoride (PVDF) were purchased Sigma Aldrich, South Korea. Potassium permanganate ($KMnO_4$), N-methyl pyrrolidone (NMP), N, N-dimethylformamide (DMF), hydrogen peroxide (H_2O_2), sulfuric acid (H_2SO_4), sodium hydroxide (NaOH), acetone (C_3H_6O), hydrazine hydrate (N_2H_4) and ethanol (C_2H_5OH) and were bought from Daejung Chemicals Ltd., South Korea. Carbon black and tetraethylammonium tetrafluoroborate ($TEABF_4$) is procured from Alfa aesar, South Korea. Table salt was purchased from Sajo supplier (South Korea).

1.2 Sonochemical reduction of graphene oxide (GO) into reduced graphene sheets (rGO):

At first, the graphene oxide (GO) sheets were prepared in accordance with the modified Hummers method (using graphite powders, $KMnO_4$ and H_2SO_4) as reported in literature.[1,2] After that, the de-oxygenation of GO sheets into reduced graphene sheets were achieved via a sonochemical process similar to that of the method reported in our earlier work.[3] Briefly, GO powders were dispersed in aqueous solution (with a concentration of 1 mg/mL) via ultrasound irradiation and the pH of the solution was adjusted into 10 using the addition of NaOH followed by the drop-wise addition of 2 mL of hydrazine hydrate solution. The ultrasound irradiation process was continued for 2 h which result in the change in brownish yellow color (GO) into black graphene sheets color indicating the de-oxygenation of GO leading to the formation of graphene sheets. Then, the resulting graphene dispersion was thoroughly washed with water and ethanol via repeated centrifugation process. Finally, the graphene sheets powders were dried at 60 °C for 12 h and used for further studies.

1.3 Fabrication and analysis of free-standing porous PVDF piezo-polymer separator

The free-standing porous PVDF films were prepared through solvent-based film casting method.[4] Briefly, 2 g of PVDF powders were dispersed in DMF solution and subjected to ultrasound irradiation process for 2 h which result in the formation of a homogeneous and transparent solution. Following this, 2.5 g of mechanically grounded table salt powders was added into the PVDF solution using the magnetic stirring process for 24 h at a temperature of 80 °C. After that, the solution was poured into a Petri dish and kept it in a hot air oven at 70 °C for overnight for removing the solvent (DMF). Then, the PVDF-table salt composite film was peeled off from the Petri dish and the salt was removed by immersing the film in deionized water for 72 h which result in the formation of porous PVDF. The prepared porous PVDF are allowed to dry at a temperature of 80 °C for 6 h and used for further characterization. The table-salt incorporated PVDF film was prepared with the addition of table salt using the similar process. The piezoelectric properties of the free-standing porous PVDF film were measured under various external mechanical forces with the aid of a linear motor (E1100), and a Keithley Electrometer (Model no: 6514) was adopted to test the short-circuit current and open circuit voltage.

1.4 Instrumentation

The crystal structure of GO and graphene sheets were obtained using an Empyrean X-ray diffractometer (XRD) instrument (Malvern Panalytical, UK) using Cu-Kα radiation (λ = 1.54184 Å). The laser Raman spectroscopy of GO, graphene (rGO) and porous PVDF were performed using Lab Ram HR Evolution Raman spectrometer (Horiba Jobin-Yvon, France, at laser excitation source of wavelength 514 nm). The morphological analysis of graphene sheets, table salt induced PVDF and porous PVDF were performed using field-emission scanning electron microscopy (TESCAN, MIRA3) under different magnifications with energy dispersive X-ray (EDS) spectroscopy. The Fourier transform infrared spectrum (FT-

IR) was measured using Thermo scientific, Nicolet-6700 FT-IR spectrometer. The chemical elements and its states were analyzed using X-ray photoelectron spectroscopy (XPS) techniques using ESCA-2000, VG Microtech Ltd, (Al Kα (1486.6 eV)).

1.5 Fabrication of self-charging supercapacitor power cell (SCSPC):

The self-charging supercapacitor power cell (SCSPC) in this work was constructed using graphene sheets as energy storage electrodes and porous PVDF incorporated $TEABF_4$ electrolyte as the separator.

1.5.1. Preparation of graphene electrodes for SCSPC:

The rGO electrodes were fabricated using the slurry coating method as described in literature.[5] Briefly, the active material (graphene), carbon black and PVDF were taken in the weight ratio of 85:10:5 and grounded well using NMP dispersant until a uniform slurry was formed. Then, the slurry was coated on stainless-steel (SS) coin cell substrate (with a dimension of 15.4 mm × 0.2 mm) using slurry coating method and allowed to dry at 70 °C in an oven overnight. The mass loading of the graphene on SS substrate is about 1 mg which was determined using the difference between the mass of graphene coated SS to that of the bare SS substrate.

1.5.2. Incorporation of $TEABF_4$ electrolyte into porous PVDF matrix:

The piezo-polymer separator used for the graphene SCSPC device was prepared by immersing the porous PVDF in a 1 M solution of $TEABF_4$ electrolyte in an argon filled glove box for 24 h. This process leads to the entrapment of electrolyte into the pores of the prepared porous PVDF and followed by drying which results in a formation solid-like piezo polymer separator films.

1.5.3. Construction of graphene based SCSPC:

The graphene based SCSPC device was fabricated in symmetric supercapacitor with coin-cell (CR2032) type configuration using two ideal graphene electrodes separated by the

solid-like piezo-polymer separator. The fabricated SCSPC device was crimped using an electric coin-cell crimping machine (MTI, Korea). All this fabrication process was performed in a glove box with less than 1 ppm of moisture and oxygen.

1.5.4. Electrochemical analysis of graphene based SCSPC:

The electrochemical performance of graphene based SCSPC device was investigated using cyclic voltammetry (CV), galvanostatic charge-discharge (CD), and electrochemical impedance spectroscopy (EIS), and long-term cyclic stability tests. The self-charging characterization of the graphene based SCSPC device was performed under an external mechanical force with the aid of a linear motor. All the electrochemical measurements were carried out using AUTOLAB PGSTAT302N electrochemical workstation. The specific capacitance (Csp), energy density (E) and power density (P) of the graphene SCSPC device were calculated using the following relations; [6–8]

$$C_{sp} = [(\int I\, dV) / (s \times \Delta V \times m)] \quad \ldots\ldots\ldots\ldots (1)$$

$$C_{sp} = [(I \times \Delta t) / (\Delta V \times m)] \quad \ldots\ldots\ldots\ldots\ldots (2)$$

$$E = (I \times \Delta t \times \Delta V) / (7.2 \times m) \quad \ldots\ldots\ldots\ldots (3)$$

$$P = (3.6 \times E) / \Delta t \quad \ldots\ldots\ldots\ldots\ldots (4)$$

Here, "C_{sp}" is the specific capacitance (F g^{-1}), "I" is the applied current (A), "ΔV" is the operating potential window, "s" is the scan rate (mV s^{-1}), "Δt" is the discharge time (s), and "m" is the combined mass of the electro-active material (g) in both electrodes.

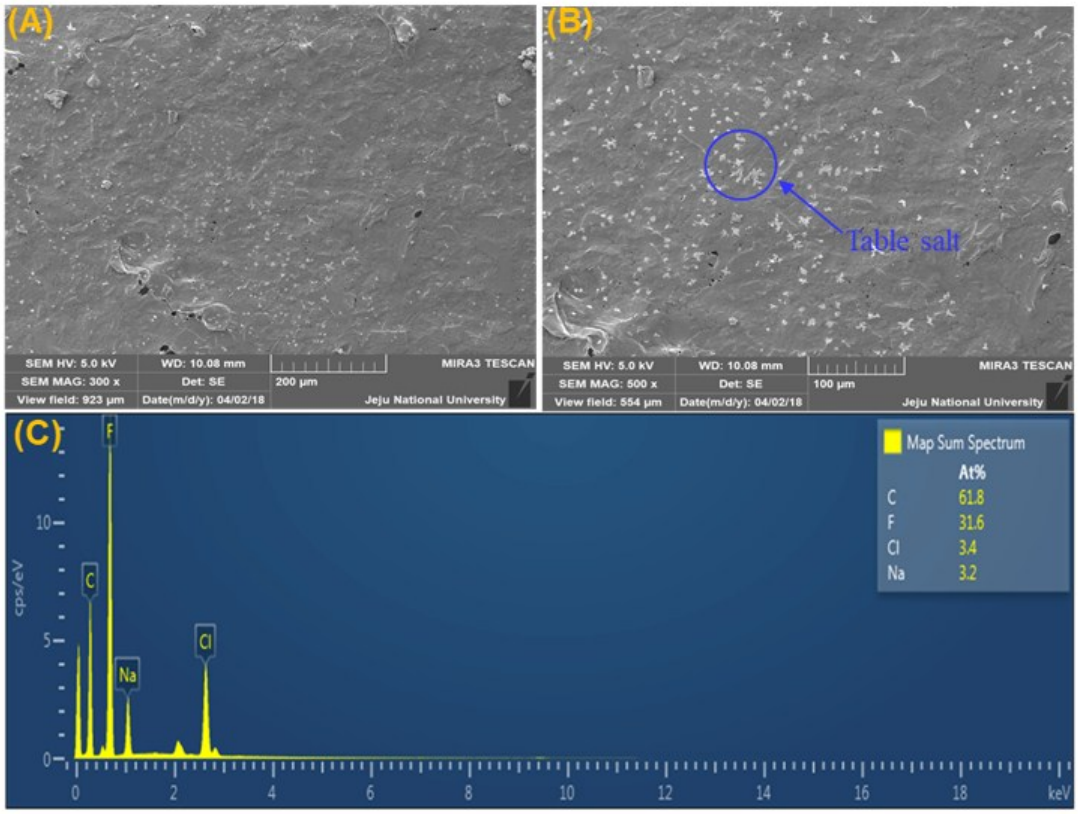

Figure S1. FE-SEM micrographs of table salt-induced PVDF film at magnification of (A) 200 µm and (B) 100 µm. (C) EDX spectrum of table salt-induced PVDF film with an atomic percentage.

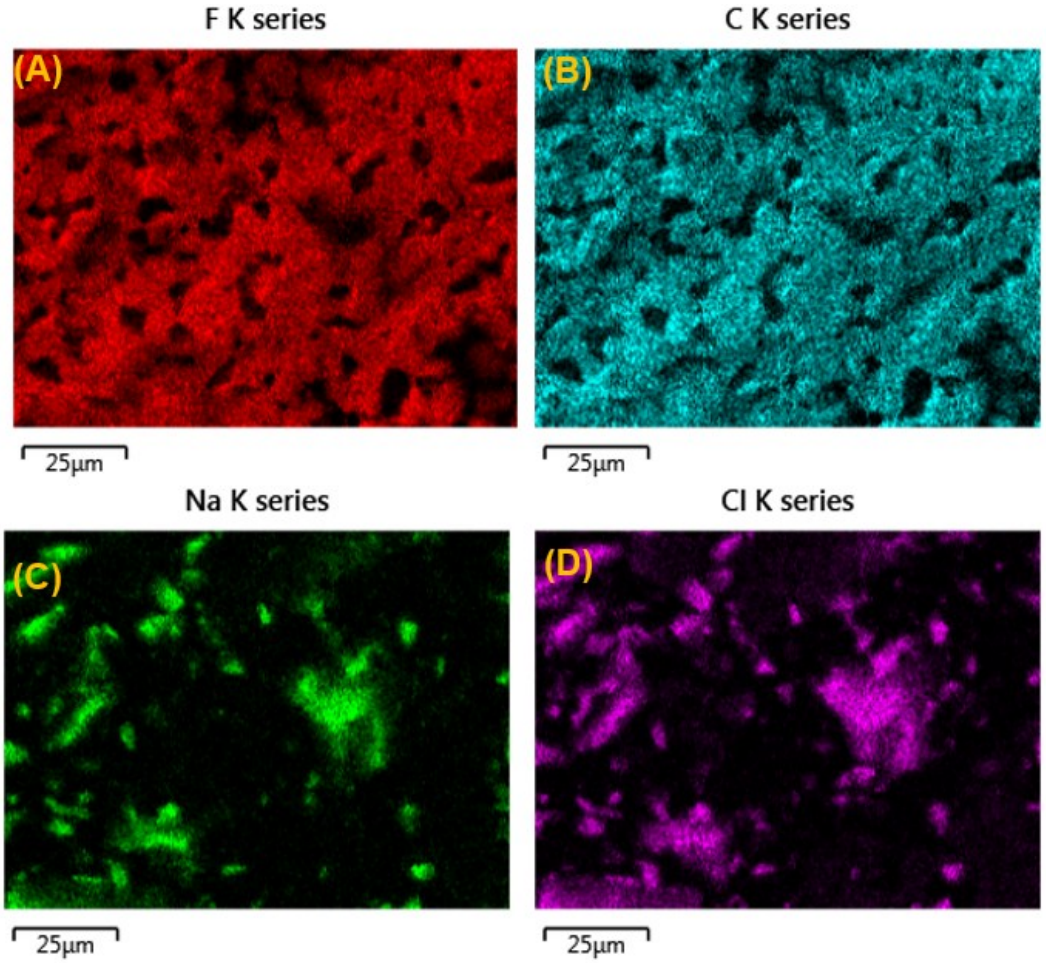

Figure S2. Elemental mapping micrographs of table salt incorporated PVDF film. The elemental maps of (A) fluorine, (B) carbon, (C) sodium and (D) Chlorine elements present in table salt incorporated PVDF film.

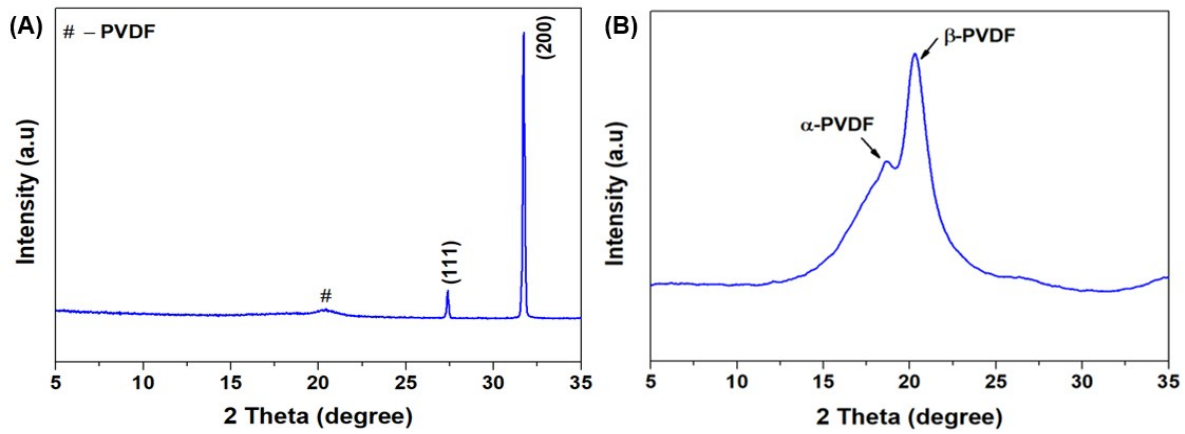

Figure S3. XRD pattern of (A) table salt incorporated PVDF film (JCPDS No:05-0628) and (B) porous PVDF film.

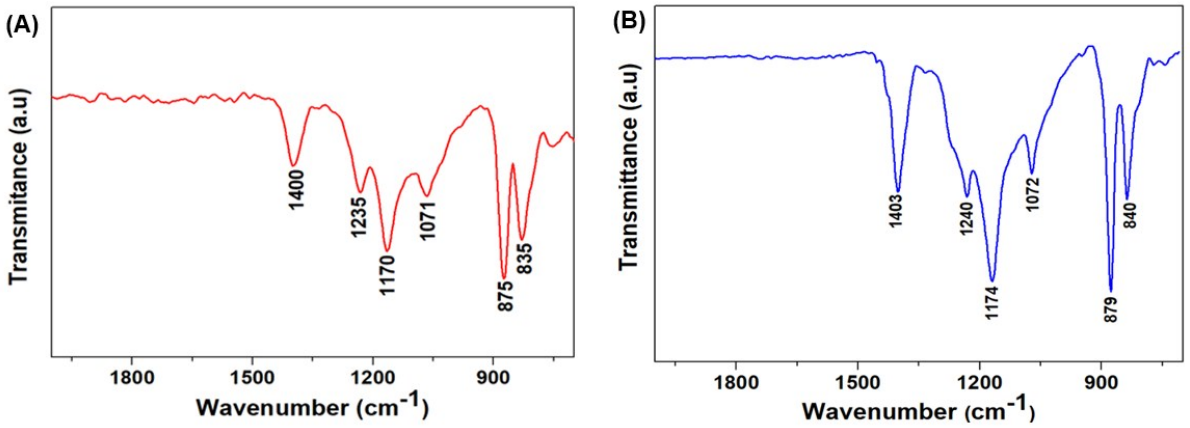

Figure S4. FT-IR spectra of (A) table salt incorporated PVDF film and (B) porous PVDF film.

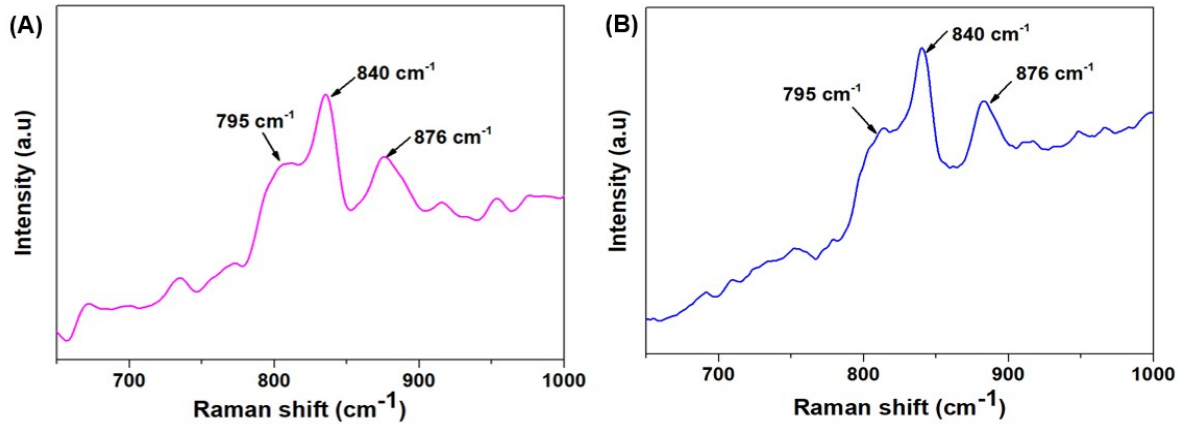

Figure S5. Raman spectra of (A) table salt incorporated PVDF film and (B) porous PVDF film.

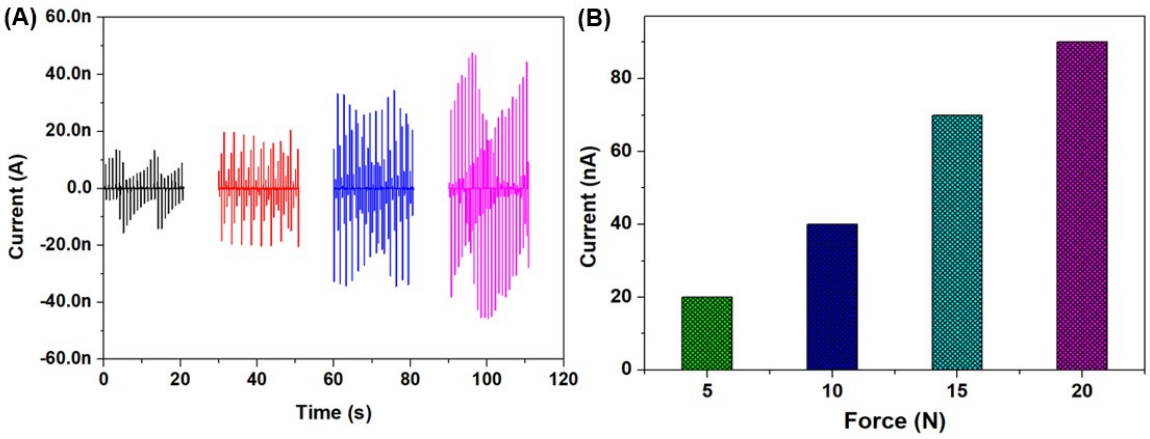

Figure S6. (A) Current profile of the porous PVDF film based nanogenerator device under various compressive forces from 5 to 20 N. (B) Variation of the output current of the porous PVDF film under different magnitude (5 to 20 N) of the applied force.

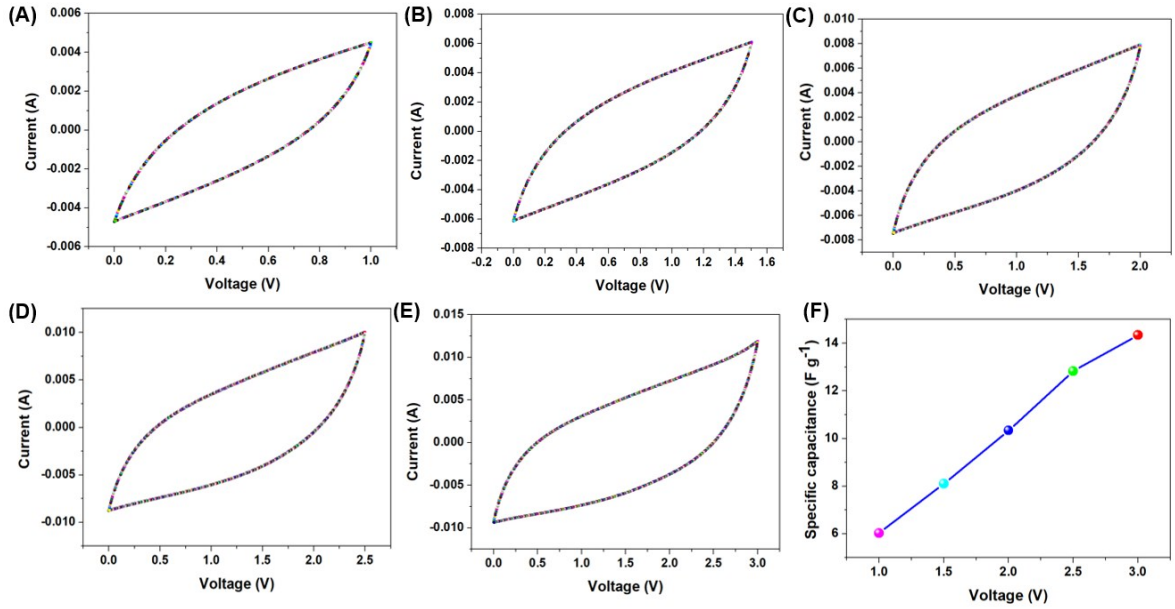

Figure S7. Electrochemical analysis of the graphene SCSPC (CR2032 coin cell) in $TEABF_4$ electrolyte. (A-E) Cyclic voltammetric profiles of the graphene SCSPC measured at the different operating potential window (1.0 to 3.0 V) using a scan rate of 200 mV s^{-1}. (F) Effect of specific capacitance of graphene SCSPC with respect to the different operating potential window (1.0 to 3.0 V).

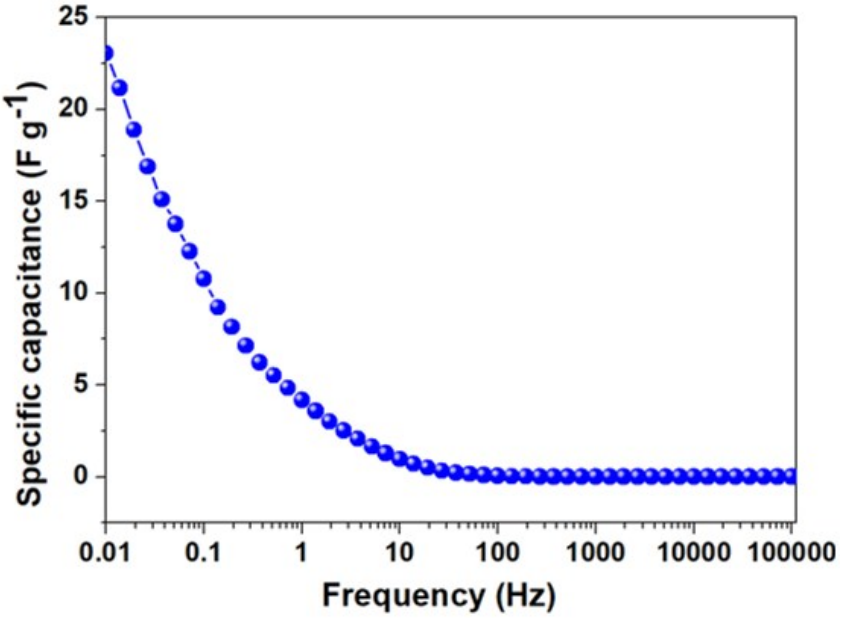

Figure S8. The plot of variation of specific capacitance of graphene SCSPC with respect to frequency.

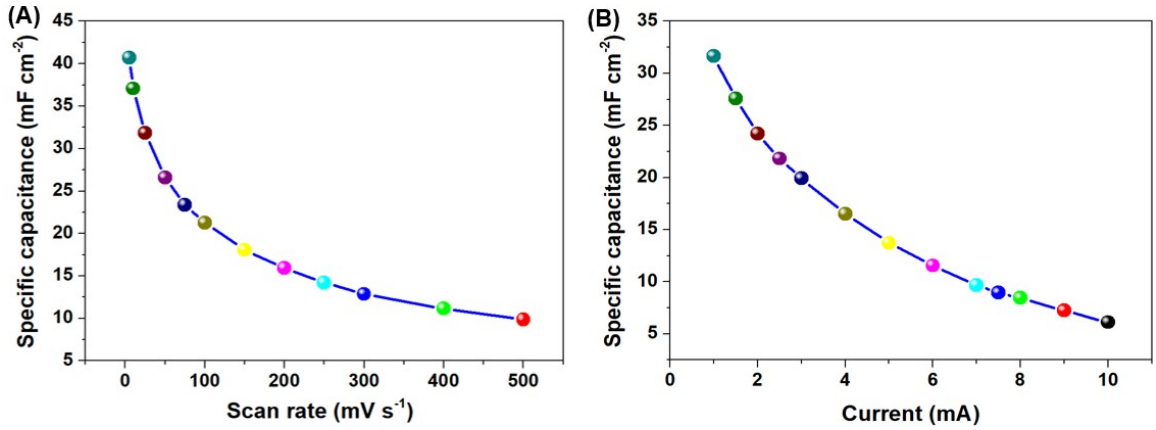

Figure S9. (A) Effect of areal specific capacitance of graphene SCSPC with respect to scan rate. (B) Effect of areal specific capacitance of graphene SCSPC with respect to the discharge current.

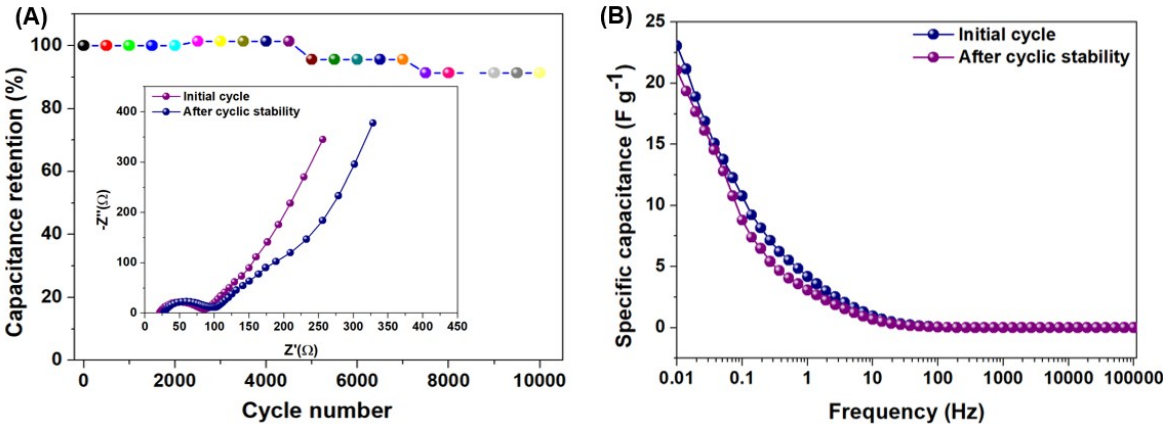

Figure S10. (A) Cyclic stability performance for graphene SCSPC over 10000 cycles with inset, shows the Nyquist plot of graphene SCSPC measured during initial and after 10000 cycle. (B) The plot of variation of specific capacitance of graphene SCSPC with respect to frequency initial and after 10000 cycles.

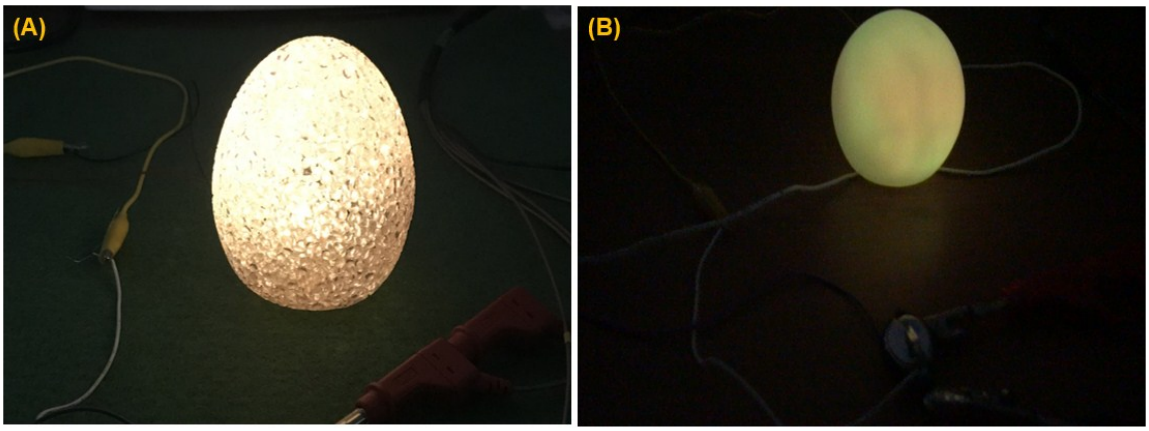

Figure S11. The practical application of fully charged graphene SCSPC to glow (A) a white LED-based night lamp, and (B) a blue LED-based night lamp.

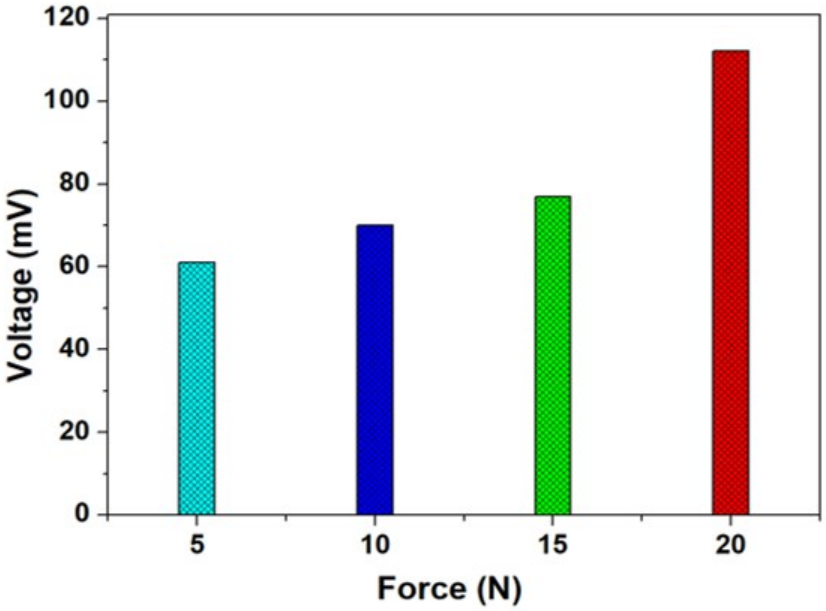

Figure S12. The effect of different applied forces on the self-charging performance of the graphene SCSPC.

Table S1. Summary of electrochemical performances of graphene SCSPC and recently reported supercapacitor devices using an ionic liquid as electrolyte.

Si. No.	Electrode material	Electrolyte	Potential window (V)	Energy density (Wh kg^{-1})	Power density (W kg^{-1})	Reference
1	HPGM	$TEABF_4$	2.5	23.5	62.5	R1[9]
2	rGO	$LiClO_4$/PC	1.6	9.4	678	R2[10]
3	rGO	$BMIBF_4$	4	16.5	1600	R3[11]
4	rGO	$[SET_3][TFSI]$-GO	2.5	17.7	875	R4[12]
5	rGO-CMK-5	$LiPF_6$	2.5	23.1	-	R5[13]
6	rGO	Et_4NBF_4	2.5	16	-	R6[14]
7	Activated carbon	$PYR_{14}TFSI$	3.5	20	2000	R7[15]
8	MoS_2 sheets	$TEABF_4$	3	18.43	1125	R8[16]
9	**rGO**	**$TEABF_4$**	**3**	**35.58**	**7500**	**This work**

References

1 K. Krishnamoorthy, M. Veerapandian, K. Yun and S.-J. Kim, *Carbon N. Y.*, 2013, **53**, 38–49.

2 S. Pei, J. Zhao, J. Du, W. Ren and H.-M. Cheng, *Carbon N. Y.*, 2010, **48**, 4466–4474.

3 K. Krishnamoorthy, G.-S. Kim and S. J. Kim, *Ultrason. Sonochem.*, 2013, **20**, 644–649.

4 F. Chen, Y. Lu, X. Liu, J. Song, G. He, M. K. Tiwari, C. J. Carmalt and I. P. Parkin, *Adv. Funct. Mater.*, 2017, **27** (41)

5 N. S. A. Manaf, M. S. A. Bistamam and M. A. Azam, *ECS J. Solid State Sci. Technol.*, 2013, **2**, M3101–M3119.

6 S. Zhang and N. Pan, *Adv. Energy Mater.*, 2015, **5**, 1401401.

7 S. Sahoo, P. Pazhamalai, K. Krishnamoorthy and S.-J. Kim, *Electrochim. Acta*, 2018, **268**, 403-410.

8 P. Pazhamalai, K. Krishnamoorthy, V. K. Mariappan, S. Sahoo, S. Manoharan and S.-J. Kim, *Adv. Mater. Interfaces*, 2018, **5**, 1800055.

9 Y. Tao, X. Xie, W. Lv, D.-M. Tang, D. Kong, Z. Huang, H. Nishihara, T. Ishii, B. Li and D. Golberg, *Sci. Rep.*, 2013, **3**, 2975.

10 Z. Liu, H. Zhang, Q. Yang and Y. Chen, *Electrochim. Acta*, 2018, **287**, 149–157.

11 Y. Chen, X. Zhang, D. Zhang and Y. Ma, *Mater. Lett.*, 2012, **68**, 475–477.

12 N. das M. Pereira, J. P. C. Trigueiro, I. de F. Monteiro, L. A. Montoro and G. G. Silva, *Electrochim. Acta*, 2018, **259**, 783–792.

13 Z. Lei, Z. Liu, H. Wang, X. Sun, L. Lu and X. S. Zhao, *J. Mater. Chem. A*, 2013, **1**,

2313–2321.

14 A. M. Navarro-Suárez, K. L. Van Aken, T. Mathis, T. Makaryan, J. Yan, J. Carretero-González, T. Rojo and Y. Gogotsi, *Electrochim. Acta*, 2018, **259**, 752–761.

15 A. Balducci, R. Dugas, P.-L. Taberna, P. Simon, D. Plee, M. Mastragostino and S. Passerini, *J. Power Sources*, 2007, **165**, 922–927.

16 P. Pazhamalai, K. Krishnamoorthy, S. Manoharan and S.-J. Kim, *J. Alloys Compd.*, 2019, **771**, 803–809.